

Theoretical Investigation and Prediction of Promising Organic Molecules for Optical and Electronic Applications

Saba Razaq Salman¹, Oday A. Al-Owaedi²

^{1, 2}Department of Laser Physics, College of Science for Women, University of Babylon, Hilla 51001, Iraq

Email: pure.saba.rasaq@uobabylon.edu.iq

Email: oday.alowaedi@uobabylon.edu.iq

Abstract

In this paper we exhibit a theoretical study using the density functional theory methods of electronic and spectral properties for a family of Oligo(phenylene-ethynylene) OPEs with pyridyl linker groups, with different transport connections para, ortho and meta. so, changing the transport connections from para to meta or ortho not only affects the intensity of the absorption, emission and emission oscillator strength but also leads to a displacement in wavelengths. On the other hand, the results of this paper prove the influence of the constructive and destructive quantum interferences on the transmission coefficient, where the changing from para to meta in the central ring for molecules PPP and MMM, caused the transmission coefficient to drop by two orders of magnitude. so, in this result the junction formation probability (JFP) of molecule OPO in prevent the electronic transport between the molecule and electrodes, which in turn increased the radiative recombination, and the later led to high emission oscillator strength value.

Keywords: The thiophene/phenylene co-oligomers, Emission Oscillator Strength, Electrical conductance

1. Introduction

One of the success stories in the field of organic optoelectronics is that of the organic light-emitting diode which has already percolated from research laboratories to household electronics [1,2]. Another promising field is that of organic field-effect transistors (OFETs), which has the potential to morph into flexible devices [3-5]. Organic light emitting transistor (OLET) combines both the electrical switching capability of OFETs and the light-generation capability of organic light-emitting diodes (OLEDs) in a single molecule device, in which the intensity and recombination zone of electroluminescence (EL) can be effectively tuned by applying gate voltage [6-9]. A successful development of OLET technology can greatly simplify the display fabrication process and lead to new applications in electrically pumped organic lasers [10-13]. and smart displays [14].

An efficient OLET should exhibit the following characteristics: a large emission oscillator strength (f_{em}), a high charge mobility, a low applied voltage, a high external quantum efficiency (EQE), and tunable recombination zone [15-17]. Moreover, effective ambipolar charge transport requires materials with proper matching of the highest occupied molecular orbital (HOMO) and lowest unoccupied molecular orbital (LUMO) energy levels with the Fermi energy level of metal electrodes. Unfortunately, strong intermolecular π - π stacking will likely quench luminescence in the solid-state. Thus, organic

systems with high solid-state emission quantum yields generally exhibit less planar, but rigid structures, which necessarily impede charge transport and result in low charge carrier mobility [18].

2. Results and Discussion

the development of new materials exhibiting proper energy level alignment, high photoluminescence quantum yield (PLQY), has become critical for further progress in this area. In this study, a family of oligo(phenylene ethynylene) (OPE) with different transport connection points para, meta, and ortho (see Figure 1.), have been proposed to investigate a new strategy depending on the quantum interference to enhance and develop the optoelectronic and thermoelectric properties.

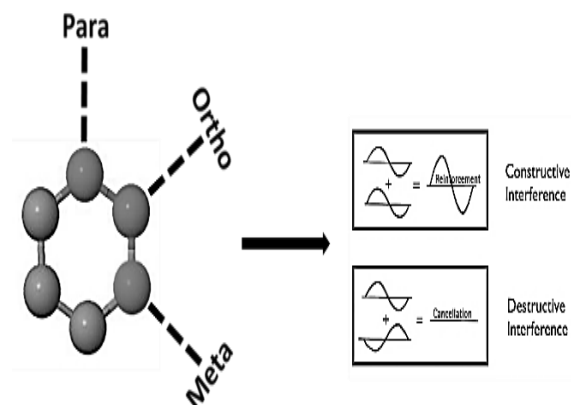


Figure 1. Constructive and Destructive Quantum Interferences via Different transport connection points.

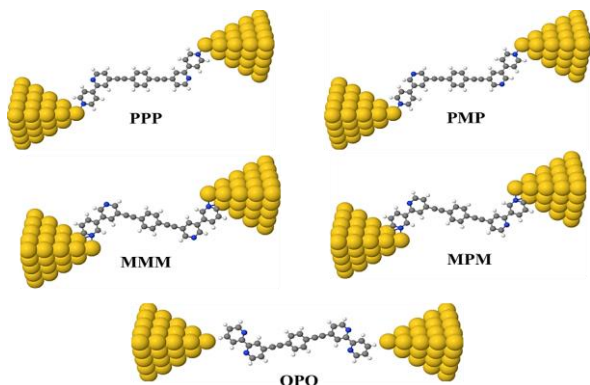


Figure 2. The optimized molecular junction of all structures.

To obtain a good insight, and to better evaluate the properties and behavior of these molecular junctions, our results for the structural, electronic and thermoelectric evolutions of the junction Au/OPE/Au are based on functional theory (DFT) calculations [19–22]. We used a PBE-GGA functional [19] and norm-conserving pseudo-potentials [23] as implemented in the SIESTA code [23,24]. Numerical atomic orbitals were used as basis sets [23]. We employed a double-zeta basis with a polarization function (DZP) for the whole system. The confining energy shift was 0.05 eV and an energy cut-off of 240 Ry was used to the grid integration. For the surface Brillouin zone (BZ) sampling we have used a (1-1-1) Monkhorst–Pack set [25]. Moreover, in our calculations the self-consistency is achieved when the change in the total energy between cycles of the SCF procedure is below 10^{-4} eV and the density matrix change criterion of 10^{-4} is also satisfied. These criteria are enough to ensure convergence in the calculated total energy of 0.05 eV. To obtain the geometries as shown in Figure 2, the supercell was such that the molecule would be connected to the two sides of the Au slab. The Au slab was modelled by a (3×3) surface unit cell and five layers of gold. In all calculations the positions of the OPE atoms and the Au atoms on the first two layers at either side were allowed to relax until the forces were smaller than 0.02 eV \AA^{-1} .

The studies of the scattering patterns of the frontier

molecular orbital (FMO) is very important to depicted the optoelectronic properties of the designed molecules because these are related to the excitation properties of the molecules. The plots of FMO's of the designed molecules including highest occupied molecular orbital (HOMO) and lowest unoccupied molecular orbital (LUMO) at the ground states (S_0) are shown in the Figure 3. Furthermore, we have investigated distribution patterns for each molecule in terms of partial density of states (PDOS) and the total density of states (TDOS) based on Mullikan population analysis. The percentage contribution of each atom in the composition of molecular orbital have been studied by using Mullikan population analysis approach as shown in Figure 4.

Figure 3. shows that the LUMOs of all molecules are extended over the backbone. The LUMOs exhibit a negligible weight on the N atoms and are therefore less delocalized than the HOMOs.

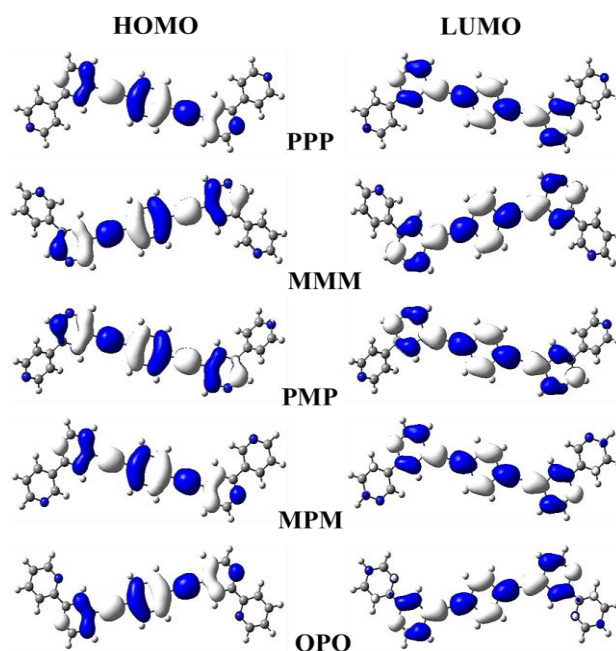


Figure 3. Iso-surfaces ($\pm 0.02 \text{ (e/bohr}^3)^{1/2}$) of the HOMOs and LUMOs.

Table 1. e_N is the number of electrons on nitrogen atoms when molecule in gas-phase. e_J is the number of electrons on nitrogen atoms when molecule in a junction. $\Gamma = e_N - e_J$ is the number of transfer electrons. HOMOs and LUMOs energies. HOMO-LUMO energy gaps.

Molecule	e_N	e_J	Γ	HOMO (eV)	LUMO (eV)	H-L Gap (eV)
PPP	28	22.09	5.91	2.63	1.2	3.83
PMP	28	25.07	2.93	2.77	1.0	3.77
MMM	28	26.02	1.98	2.8	0.96	3.73
MPM	28	21.05	6.95	1.93	1.35	3.28
OPO	28	18.87	9.13	2.04	0.75	2.79

Table 1. shows HOMO and LUMO energies and energy gaps between HOMO and LUMO all designed molecules. The trend for HOMO-LUMO energy gaps is PPPH-Lgap > PMPH-Lgap \geq MMMH-Lgap > MPMH-Lgap > OPOH-Lgap. The smaller energy gap is observed for OPO molecule (2.79 eV). These results could be interpreted in terms of a high electronegativity of the carbon atoms in the

backbone of the molecule, so it enhance the delocalization of pi-electrons by pulling the electron density from the side group, and therefore an increase in HOMO energy and pronounce increase in LUMO energy is observed. Depending on this, the difference in the HOMO-LUMO gap value of these molecules may be ascribed to the different position of the donor atoms (Nitrogen atoms), which may led to a difference in the value of the electronegativity.

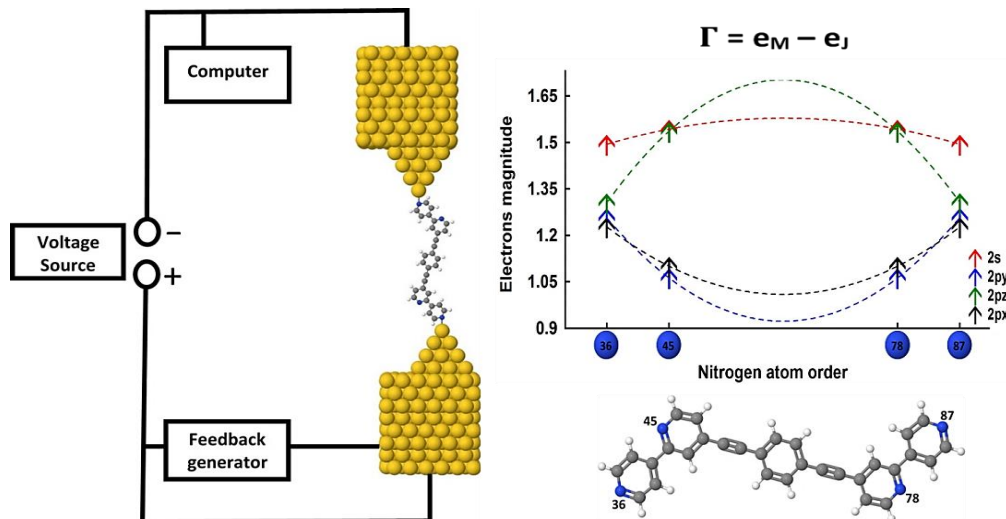


Figure 4. Theoretical model of electrons transfer based on Mulliken population analysis approach.

Figure 4. exhibits a simple theoretical model of the transfer electrons (Γ) between the molecule atoms themselves, and on onthor hand, between the

molecule and electrodes as shown in Table 1 and Figure 4, based on Mulliken population analysis approach.

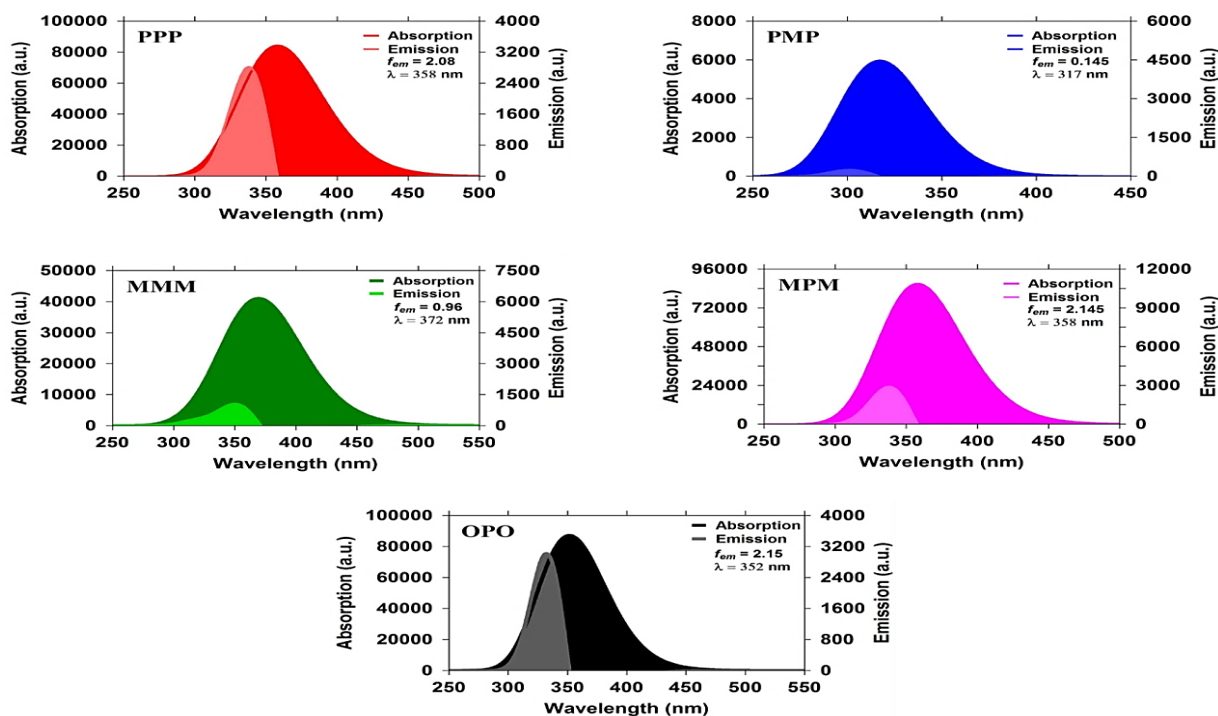


Figure 5. Represents the absorption, emission and emission oscillator strength of all molecules.

Figure 5. shows that the absorption intensity fluctuated dramatically, since its value was 84248 a.u. for the molecule PPP, with three para transport connection points, then it decreased sharply to 40809 a.u. for the molecule MMM, with with three meta connection points. The lowest value (5964 a.u.) of the absorption intensity is presented by PMP molecule, whereas the highest value (87102 a.u.) introduced via OPO molecule. In addition, it could be observed that the maximum wavelength (λ_{max}) for all molecules lies in the visible region, and there is also a fluctuation from 317 nm for PMP to 372 nm for MMM. of 365.4 nm. Based on these results, we can conclude that changing the transport connections from para to meta or ortho not only affects the intensity of the absorption, but also leads to a displacement in wavelengths.

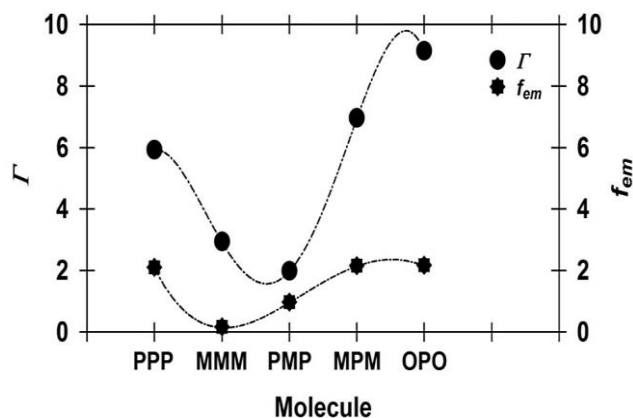


Figure 6. The transferred electrons from molecule (Γ), and the emission oscillator strength (f_{em}) of all molecules.

The second important result is exhibited in figures 5. and 6., and Table 2. which is the emission oscillator strength (f_{em}), and its relationship with the electron transfer and transport connection points. The molecules with para connection in the central part of

molecule, PPP, MPM and OPO produce the highest f_{em} (2.08, 2.145 and 5.15 respectively), while the molecules with meta connection in the central part of molecule, MMM and PMP, show the lowest f_{em} (0.154 and 0.145 respectively).

Table 2. Emission strength oscillator (f_{em}). Maximum wavelength (λ_{Max}). Absorption intensity (A). Emission intensity (E).

Molecule	f_{em}	λ_{Max} (nm)	A (a.u.)	E (a.u.)
PPP	2.08	358	84248	2819
PMP	0.145	317	5964	251
MMM	0.154	316	40809	1036
MPM	2.145	358	86884	2911
OPO	2.15	352	87102	3019

The order of emission and absorption intensities and the emission oscillator strength (f_{em}) is OPO > MPM > PPP > MMM > PMP. These results can formulate for us a promising theoretical strategy for choosing the structures and materials that can serve as an active laser medium. Since, the emission cross section (σ_{em}) of a laser transition is considered an important parameter, because it can impact the accomplishment of laser in terms of the threshold energy, output energy, maximum gain, etc. [26]. In other words, the high value of emission cross section (σ_{em}) leads to high gain laser, and since it is a direct proportion between the emission cross section and the emission oscillator strength. Therefore, our theoretical strategy to enhance the emission via change the transport connection points of molecules can be a powerful way to develop the laser technique.

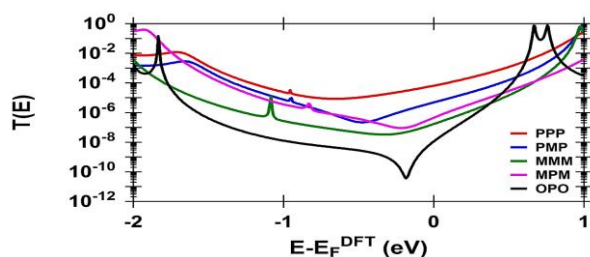


Figure 7. Represents the transmission coefficient as a function of the electron's energy of all molecular junctions.

Charge transport characteristics of single-molecule junctions formed from the molecules in Figure 7, were investigated using GOLLUM code [27] to simulate scanning tunnelling microscopy (STM) technique.

Figure 7 displays the transmission coefficient $T(E)$ versus the electron's energy of molecule PPP, PMP, MMM, MPM and OPO. The highest value (6.73×10^{-5}) of $T(E)$ is presented via PPP molecule, which could be assigned to a perfect formation of the single-molecule junction. Significant differences of $T(E)$ are observed for other molecules, as shown in Figure 7 which are ascribed to the variety of connectivities of the central ring (see Figure 2) and locations of the nitrogen in the anchor units, while for molecule PPP, the para connection in both central and terminal rings, which leads to the highest transmission coefficient. As shown in Table 3. and Figure 7, the lowest value (1.26×10^{-8}) of $T(E)$ is exhibited by OPO molecule. These results could be understood in terms of the junction formation probability (JFP), since JFP is 100% for molecules PPP, PMP, MMM and MPM. Whereas, for OPO molecule the JFP decreased sharply to almost zero, and there is no junction as shown in Figure 2, because Nitrogen (N) atoms in the terminal ortho pyridyl is partially hidden from the electrode surfaces and therefore it is difficult to form a bridge between the two gold electrodes.

Table 3. L (N...N), is the molecule length, D (Au...Au), is the molecular length. X is the bond length (Au...N). Z (D - 0.25), is the theoretical electrodes separation. T(E) is the transmission coefficient.

Molecule	L (nm)	D (nm)	X (nm)	Z (nm)	T(E)
PPP	2.19	2.6	0.23	2.35	6.73×10^{-5}
PMP	2.19	2.6	0.23	2.35	5.02×10^{-6}
MMM	1.97	2.14	0.23	1.89	1.76×10^{-7}
MPM	1.97	2.14	0.23	1.89	4.43×10^{-7}
OPO	1.7	2.87	0.23	2.62	1.26×10^{-8}

Table 3 shows that theoretical electrode separations (Z) follow the trends $Z_{OPO} > Z_{PPP} = Z_{PMP}$ and $Z_{MMM} = Z_{MPM}$ that correlate with the molecular L distance, demonstrating that the gold-anchor link is primarily controlled by the gold-nitrogen bonds. Therefore, it is clear that changes in the position of the N atom within the anchors affects both the JFP, as well as the

transmission coefficient as shown in Figure 7. Unlike the PPP molecule, the other molecules possess anchoring nitrogen atoms located at meta or ortho positions within the terminal rings that do not naturally bind to electrode surfaces, as shown in Figure 2.

Another result has been reflected from Figure 7 which is worth mentioning that the changing from

para to meta in the central ring for molecules PPP and MMM, caused the transmission coefficient to drop by two orders of magnitude, and these results are consistent with previous studies [28,29,30,31]. On the other hand, the terminal ring of the MPM molecule reduces $T(E)$ by an order of magnitude in comparing with that of PMP molecule. Thus, this study demonstrated the important contribution of constructive and destructive quantum interferences in the terminal and central aromatic rings to the transmission coefficient, which in turn with a collaboration of the JFP affected the electrons transfer factor (Γ), which influenced the radiative recombination, and the latter impacted strongly the emission oscillator strength (f_{em}) and led to the results presented in figures 5 and 6.

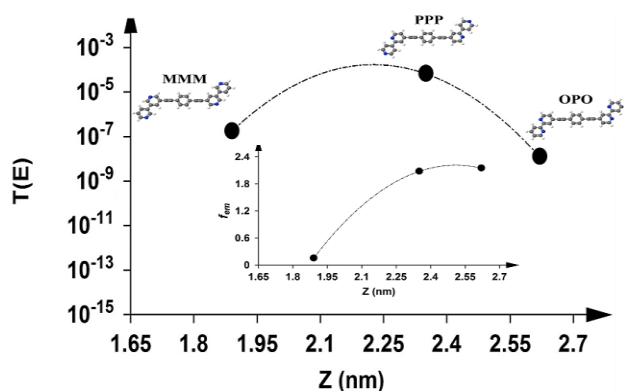


Figure 8. Represents the transmission coefficient $T(E)$ as a function of the theoretical electrodes separation (Z) of the molecules PPP, MMM and OPO. The insert figure shows the emission oscillator strength (f_{em}) as a function of Z for the same molecules.

The results shown in Figure 8. illustrate the confusion that may appear to the reader regarding the previous results of the molecules OPO and MMM for their transmission coefficient and emission oscillator strength values. First of all, the OPO molecule has the highest f_{em} and the lowest $T(E)$, and this result in fact confirms an important role of the junction formation probability (JFP) in prevent the electronic transport between the molecule and electrodes, which in turn increased the radiative recombination, and the later led to high emission oscillator strength value. On the other hand, the ortho and para connectivities of OPO molecule create a constructive quantum interference, which improves significantly the electronic transport between its atoms, which for sure increased the emission intensity (3019 a.u.) of this molecule, as shown in Table 2. and Figure 5.

In contrast, Figure 8. shows the molecule MMM with meta connectivities possess the lowest f_{em} , and $T(E)$. This result indicates to the effective influence of the destructive quantum interference in block the electroinc transport between molecule atoms, as well as between molecule and electrodes. As a consequence, the emission intensity (1036 a.u.) was very low, as shown in Table 2. For PPP molecule with para connectivities, the high junction formation probability (JFP) and the constructive quantum interference aided to increase both the transmission

coefficient and the emission strength oscillator. Finally, these result bring us to an important fact that those molecules could be powerful for the optoelectronic applications such as light emitting diodes.

3. Conclusions

We exhibites a theoretical study using the density functional theory methods of electronic and spectral properties for a family of Oligo(phenylene-ethynylene) OPEs with pyridyl linker groups, with different transport connections para, ortho and meta. Based on the results that have been presented in this section, we can conclude that changing the transport connections from para to meta or ortho not only affects the intensity of the absorption, emission and emission oscillator strength but also leads to a displacement in wavelengths. Since, the molecules with para connection in the central part of molecule, PPP, MPM and OPO produce the highest f_{em} , while the molecules with meta connection in the central part of molecule, MMM and PMP, show the lowest f_{em} , as well as the maximum wavelength (λ_{max}) for all molecules lies in the visible region, and there are fluctuations depends on the connection transport point of the molecule.

On the other hand, the results of this section prove the influne of the constructive and destructive quantum interferences on the transmission coefficient, where the changing from para to meta in the central ring for molecules PPP and MMM, caused the transmission coefficient to drop by two orders of magnitude. Furthermore, it could be concluded that there is an important role of the junction formation probability (JFP) of molecule OPO in prevent the electronic transport between the molecule and electrodes, which in turn increased the radiative recombination, and the later led to high emission oscillator strength value.

References

- [1] D. Zhang, Huang, T., Duan, L. Emerging Self-Emissive Technologies for Flexible Displays. *Adv. Mater.* 2020, 32: p. 1902391.
- [2] A. J. Heeger, Semiconducting and Metallic Polymers: The Fourth Generation of Polymeric Materials (Nobel Lecture). *Angew.Chem., Int. Ed.* 2001, 40: p. 2591–2611.
- [3] H. Sirringhaus, 25th Anniversary Article: Organic Field-Effect Transistors. The Path Beyond Amorphous Silicon. *Adv. Mater.* 2014. 26: p.1319–35.
- [4] Y. Zhao, Guo, Y.; Liu, Y. 25th Anniversary Article. Recent Advances in N-Type and Ambipolar Organic Field-Effect Transistors. *Adv. Mater.* 2013. 25: p.5372–91.
- [5] Y. Ren, Yang, X.; Zhou, L.; Mao, J. Y.; Han, S. T.; Zhou, Y. Recent Advances in Ambipolar Transistors for Functional Applications. *Adv. Funct. Mater.* 2019. 29: p.1902105.

- [6] C. Zhang, Chen, P.; Hu, W... Organic Light-Emitting Transistors: Materials, Device Configurations, and Operations. *Small* 2016. 12: p.1252–94.
- [7] Liu, C. F.; Liu, X.; Lai, W. Y.; Huang, W. Organic Light-Emitting Field-Effect Transistors: Device Geometries and Fabrication Techniques. *Adv. Mater.* 2018.30: p.1802466.
- [8] J.Zaumseil, Recent Developments and Novel Applications of Thin Film, Light-Emitting Transistors. *Adv. Funct. Mater.* 2020. 30: p.1905269.
- [9] A. Hepp, H. Heil, Weise, W.; Ahles, M.; Schmechel, R.; von Seggern, H. Light-Emitting Field-Effect Transistor Based on a Tetracene Thin Film. *Phys. Rev. Lett.* 2003. 91: p.157406.
- [10] S. Toffanin, Capelli, R.; Koopman, W.; Generali, G.; Cavallini, S.; Stefani, A.; Saguatti, D.; Ruani, G.; Muccini, M. Organic Light-Emitting Transistors with Voltage-Tunable Lit Area and Full Channel Illumination. *Laser & Photonics Reviews* 2013. 7: p. 1011–1019.
- [11] W. A. Koopman, Natali, M.; Donati, G. P.; Muccini, M.; Toffanin, S... Charge–Exciton Interaction Rate in Organic Field-Effect Transistors by Means of Transient Photoluminescence Electromodulated Spectroscopy. *ACS Photonics* 2017. 4: p.282–291.
- [12] A. S. D. Sandanayaka, Matsushima, T.; Bencheikh, F.; Terakawa, S.; Potschavage, W. J.; Qin, C.; Fujihara, T.; Goushi, K.; Ribierre, J.-C.; Adachi, C. Indication of Current-Injection Lasing from an Organic Semiconductor. *Appl. Phys. Express* 2019. 12: p. 061010.
- [13] Liu, D.; De, J.; Gao, H.; Ma, S.; Ou, Q.; Li, S.; Qin, Z.; Dong, H.; Liao, Q.; Xu, B.; Peng, Q.; Shuai, Z.; Tian, W.; Fu, H.; Zhang, X.; Zhen, Y.; Hu, W. Organic Laser Molecule with High Mobility, High Photoluminescence Quantum Yield, and Deep-Blue Lasing Characteristics. *J. Am. Chem. Soc.* 2020. 142: p.6332–6339.
- [14] L. Hou, Zhang, X.; Cotella, G. F.; Carnicella, G.; Herder, M.; Schmidt, B. M.; Patzel, M.; Hecht, S.; Cacialli, F.; Samori, P. Optically Switchable Organic Light-Emitting Transistors. *Nat. Nanotechnol.* 2019. 14: p.347–353.
- [15] D. Yuan, Sharapov, V.; Liu, X.; Yu, L. Design of High- Performance Organic Light-Emitting Transistors. *ACS Omega* 2020. 5: p.68.
- [16] C. J. Lambert, Liu, S.-X. *Chem. Eur. J.* 2018, 24, 4193-4201; K.Yoshizawa, T. Tada, and A. Staykov, *J. Am. Chem. Soc.* 2008. 130: p.9406
- [17] R. Stadler, Jacobsen, K. W. *Phys. Rev. B* 2006. 74: p.161405.
- [18] S. Huzinaga and S. Narita. Mulliken Population Analysis and Point Charge Model of Molecules. *Israel Journal of Chemistry* 1980. 19: p. 242-254.
- [19] Peng, Q., Yi, Y., Shuai, Z. & Shao, J. Toward quantitative prediction of molecular fluorescence quantum efficiency: role of duschinsky rotation. *J. Am. Chem. Soc.* 2007. 129: p. 9333–9339.
- [20] P. Hohenberg and W. Kohn, *Phys. Rev.*, 1964. 136: p. B864–B871.
- [21] W. Kohn and L. J. Sham, *Phys. Rev.*, 1965. 140: p. A1133–A1138.
- [22] K. Capelle, *Braz. J. Phys.*, 2006. 6: p.1318–1343.
- [23] J. P. Perdew, K. Burke and M. Ernzerhof, *Phys. Rev. Lett.*, 1996. 77: p. 3865–3868.
- [24] N. Troullier and J. L. Martins, *Phys. Rev. B: Condens. Matter Mater. Phys.*, 1991. 43: p.1993–2006.
- [25] P. Ordejo'n, E. Artacho and J. M. Soler, *Phys. Rev. B: Condens. Matter Mater. Phys.*, 1996.53: p. R10441–R10444.
- [26] D. Sa'nchez-Portal, P. Ordejo'n, E. Artacho and J. M. Soler, *Int. J. Quantum Chem.*, 1997. 65: p.453–461.
- [27] E. Artacho, D. Sa'nchez-Portal, P. Ordejo'n, A. Garcia and J. M. Soler, *Phys. State Solid. B*, 1999. 215: p. 809–817.
- [28] H. J. Monkhorst and J. D. Pack, *Phys. Rev. B: Solid State*, 1976.13: p. 5188–5192.
- [29] J Ferrer, C J Lambert, V M García-Suárez, D Zs Manrique, D Visontai, L Oroszlany, R Rodríguez-Ferradás, I Grace, S W D Bailey, K Gillemot, Hatef Sadeghi and L A Algharagholy,. "GOLLUM: a next-generation simulation tool for electron, thermal and spin transport." *New Journal of Physics*, 2014.16 (9): p.93029.
- [30] S. V. Aradhya, et al. Dissecting contact mechanics from quantum interference in single-molecule junctions of stilbene derivatives. *Nano Lett.* 2012. 12: p. 1643–1647.
- [31] C. R. Arroyo, et al. Signatures of quantum interference effects on charge transport through a single benzene ring. *Angew. Chem. Int. Ed.* 2013. 52: p.3152–3155.